Ground Vibration Caused by Tunnel Construction and its Effect on an Electron Microscope

Jun Tobita[1], Nobuo Fukuwa[2]

[1]Associate Professor, Graduate School of Environmental Studies, Nagoya University
[2]Professor, Graduate School of Environmental Studies, Nagoya University

Abstract

In this study, we observed the vibrations caused by the construction of a roadway tunnel excavated using the New Austrian Tunneling Method (NATM) in an urban area. We analyzed the resulting vibrations and disturbances and their effect on a high-voltage electron microscope (HVEM). The characteristics of the construction equipment, various construction tasks, wave propagation and attenuation in the soil, along with the transmission of vibration forces to adjacent buildings were also clarified. These findings were combined and the effects on the HVEM were examined to model vibration-induced disturbances. The accuracy of these findings was confirmed by comparing the results obtained with actual observations that were recorded later. The findings of this study are expected to enhance the ability to distinguish between the many factors involved in vibration-induced disturbances caused by equipment. The findings could also be applied to monitoring construction activities and predicting the effects of vibration-induced disturbances on high-precision equipment.

1. Introduction

When constructing underground structures such as subway and roadway tunnels, it is essential to investigate the influence on surface structures resulting from tunnel construction and its related noise and vibration. A greater understanding of these phenomena is particularly valuable in urban areas. Furthermore, buildings today often house high-precision equipment that can be affected by even low levels of vibration. The characteristics of vibrations arising from tunneling operations are strongly influenced by the tunneling method used, the soil conditions of the area, and the structures of nearby buildings (Takemiya, ed., 2005, Takei et al., 2008).

In order to model vibrations and determine ways in which they can be counteracted and mitigated, it will be necessary to separately consider the characteristics of each of the different processes occurring in actual tunneling operations. Examples of these parameters include vibrations occurring as a result of the equipment employed and operation techniques, classification of the wave propagation in the ground and ground wave attenuation with distance, vibration imposed on adjacent buildings, and the effects imposed on high-precision equipment.

Using extensive vibration measurements that were collected during tunneling operations, this paper clarifies the characteristics of vibrations transmitted through the soil during expressway tunneling excavations in an urban area. The study focuses on the effects of these vibrations on nearby buildings and on a typical high-precision instrument (a high-voltage electron microscope (HVEM), H-1250ST, 1,000 kV, CTEM/STEM). The vibration measurements were carried out using a large array of sensors that were placed at various locations inside the tunnel, buried in the ground, installed in the building housing the HVEM and attached to the HVEM itself. Closed circuit television (CCTV) cameras were installed to simultaneously observe tunneling operating conditions and the HVEM monitor in order to provide additional information about the relations between tunneling operations, vibrations, and disturbances to the instrument. We then attempted to predict the vibration characteristics that would occur as the tunnel-boring machine passed directly beneath the HVEM, and subsequently compared these modeled predictions with the results of actual observations. These findings indicated that the present approach for modeling vibrations resulting from underground construction operations is effective.

Contact Author: Jun Tobita, Associate Professor, Graduate School of Environmental Studies, Nagoya University, Furo-cho, Chikusa-ku, Nagoya 464-8601, Japan.
Tel: +81-52-789-3754, Fax: +81-52-789-3768
e-mail: tobita@sharaku.nuac.nagoya-u.ac.jp

2. Outline of Tunneling Operations and Vibration Measurements

This study monitored a tunneling project conducted beneath the northern end of the Higashiyama Campus of Nagoya University that will eventually form part of a Nagoya metropolitan expressway. The New Austrian Tunneling Method (NATM) was used to construct a tunnel with a limited thickness of covering soil and a wide cross-section. The surface area above and on either side of the tunnel consists of a residential district and various university research facilities employing high-precision equipment, including an HVEM laboratory; however, it is feared that the vibrations caused by the tunneling and tunnel traffic could disrupt activities at those research facilities.

Figure 1 shows the general plan and cross-sectional views of the tunnel and nearby university structures. The tunneling operation proceeded from west to east (left to right in the figure). First, two smaller tunnels (known as drifts) were excavated on each side of the proposed path of the main bore, which was excavated between the drifts. The area consists of soft topsoil from the surface to −5 m, sand and gravel from −5 m to the upper half of the tunnel (about −15 m), and clay and sand below that level. The pilings of the nearby buildings are supported by a layer of hard sand and gravel.

Measurements were carried out in the adjacent structures and in the soil along Transects A, B and C during the tunneling progress. The measurements along Transect C provided data related to the building

where the most precise HVEM maintained in this complex was located. At its closest, the straight-line distance from the building to the tunnel was about 25 m.

Vibration sensors were placed in the tunnel, buried underground, installed at ground level, and at sensor points located in the building. (Surface and underground points are shown by open and closed circles, respectively.) The sensors used were servo-type accelerometers on Transects A and C (Fukuwa et al. 1997) and temporary moving-coil type microtremor sensors on Transect B (see section 4 below).

Figure 1(d) shows a close-up view of the HVEM and its vibration isolation table, which is supported with rubber bearings and viscous dampers. Sensor C6 was on the table. The mass foundation of the isolation device is supported by 12 piles measuring 9 m within the dense gravel layer.

Closed circuit TV cameras were placed in the tunnel and at the HVEM so that both locations could be observed simultaneously in a split image on a single monitor. Photo 1 shows the monitor screen. The upper images show the tunnel interior, the lower left image shows vibrations in the tunnel and in the soil, and the lower right image shows the screen of the HVEM. These streaming images were recorded and will be used for further investigation into vibrations produced by activities and equipment employed during tunnel construction, and to determine how these factors affect HVEM operation.
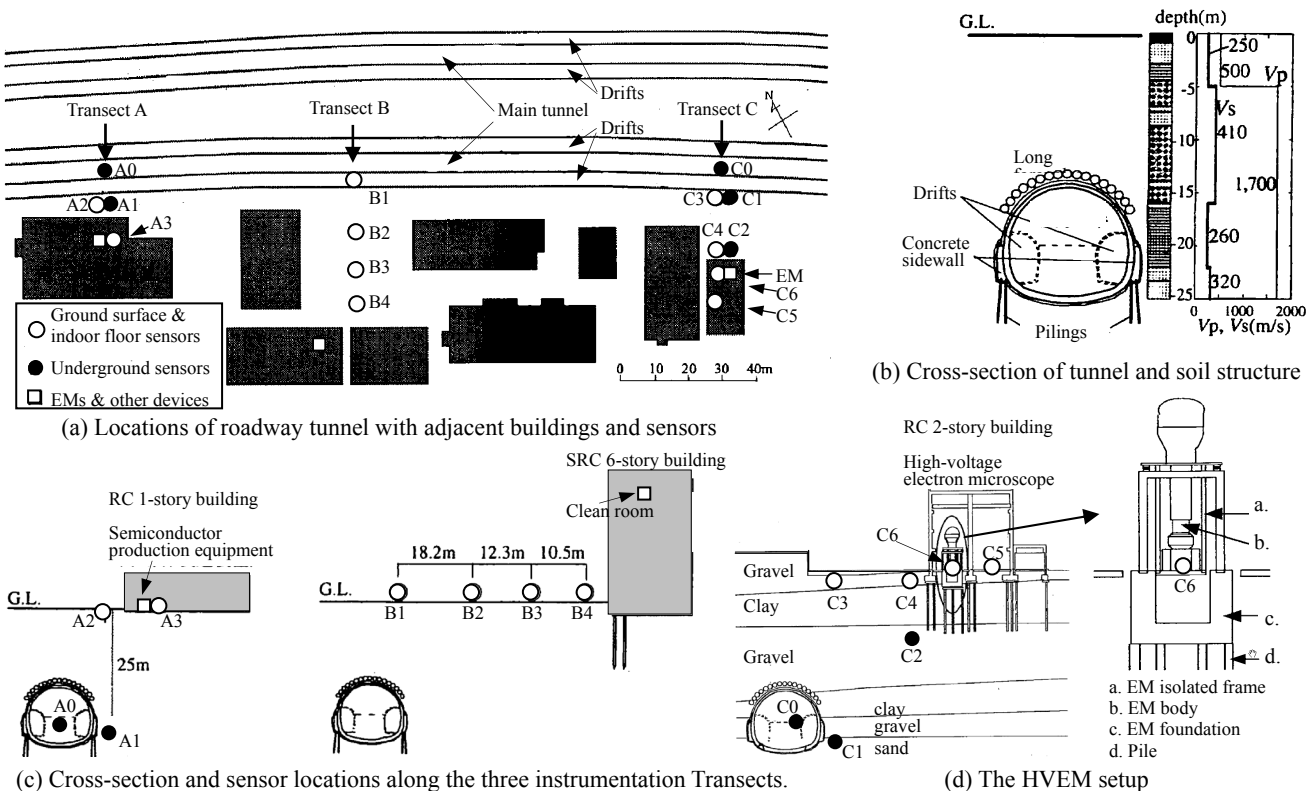

(a) Locations of roadway tunnel with adjacent buildings and sensors

(b) Cross-section of tunnel and soil structure

(c) Cross-section and sensor locations along the three instrumentation Transects.

(d) The HVEM setup

Fig.1. Outline of the tunnel project, nearby buildings, HVEM setup, and the sensor networks

Photo 1. Split screen showing tunnel construction activities, seismic waveform and electron microscope monitor

3. Characterization of Vibrations Caused by Tunneling Equipment

The vibrations caused by various kinds of tunneling equipment were compared by conducting observations along Transect C, immediately adjacent to the tunnel. Figure 2 shows the three kinds of heavy equipment during operation and their accompanying vibration records. The oval circles on parts of the vibration record indicate the vibrations caused by equipment. It was not possible to determine which equipment was being used solely by looking at the raw vibration data. However, observations from the CCTV camera installed in the tunnel (as mentioned in Section 2 and shown in Photo 1) enabled the observer to identify the equipment being used. Figure 3 presents the Fourier spectra of the different operations at the A1 sensor.
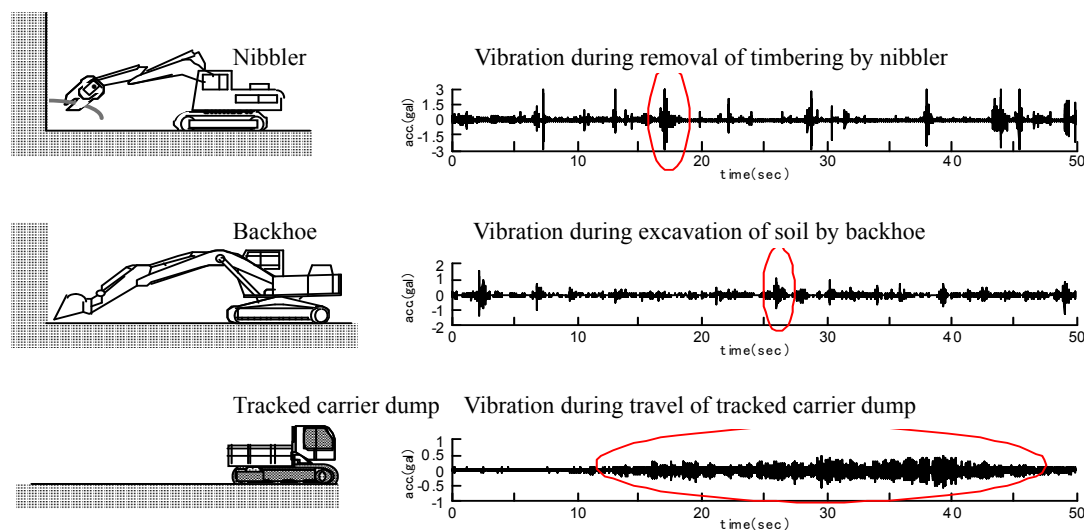

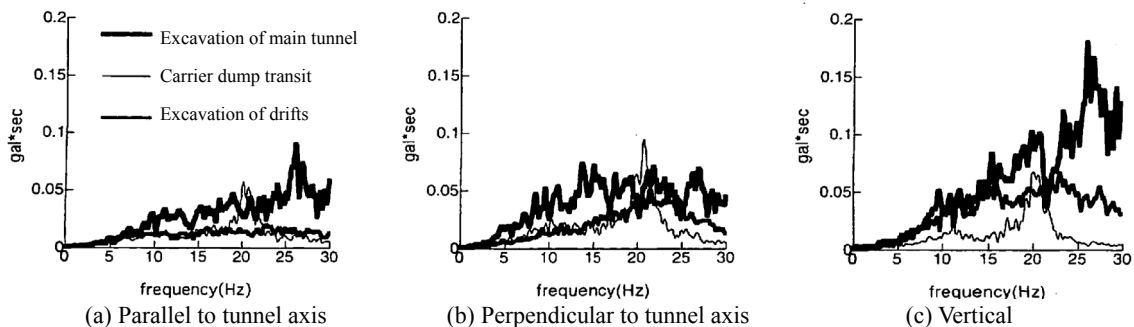Fig.2. Characteristics of vibration caused by different construction equipment

(a) Parallel to tunnel axis   (b) Perpendicular to tunnel axis   (c) Vertical

Fig.3. Acceleration spectra during equipment operation along Transect A (Sensor A1)

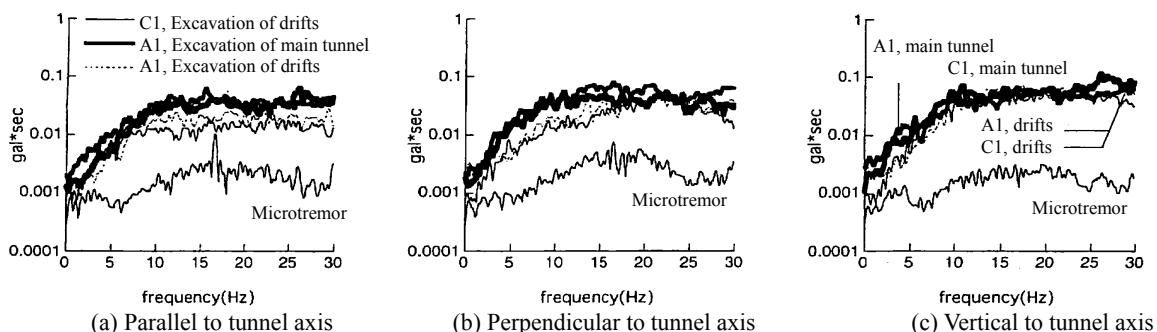(a) Parallel to tunnel axis   (b) Perpendicular to tunnel axis   (c) Vertical to tunnel axis

Fig.4. Acceleration spectra during excavation of drifts and main tunnel measured at Transects A (A1) and C (C1)

These spectra provided clear indications of both the equipment in use and the difference of vibration characteristics along three axes.

For example, pulse-like vibrations caused by excavation (Fig. 2) show wide frequency range in Fig. 3. Alternatively, long duration noises caused by the tracked carrier dump (which is a dump truck equipped with caterpillar tracks, as shown in Fig. 2) have relatively low amplitude even though a clear peak exists at around 20 Hz. As a similar peak appears at different frequencies depending on the traveling velocity and ground surface conditions in the tunnel, it was considered likely that the peak was caused by high frequency mechanical noises, most likely emitted from the caterpillar tracks of heavy construction equipment traveling over rough surfaces.

Figure 4 provides comparisons of the vibrations observed on Transects A and C during excavation of the drifts and the subsequent main tunnel. The vibrations were more intense during the digging of the main tunnel, although the spectra were relatively similar since the construction equipment activities

were similar. The vibration characteristics obtained along Transects A and C during the operation of other earthmoving equipment were both similar. It is apparent that digging resulted in vibrations more than 10 times as intense as those experienced when the equipment was not in use.

The long-term observations of the tunneling operations showed that the amplitude and frequency were generally constant for all vibrations. The results of these measured vibration characteristics can be used when observing other projects of this type in the future.

4. Wave Propagation in Soil

We will now examine how the distinctive components of the most common vibrations described in the previous section propagate through the soil. Figure 5 shows the waveforms and three-dimensional (3D) orbits of particles at points B1 – B4 on the ground surface along Line B. These are examples of records taken at the location marked with × near point B1 during excavations 23 m below ground level. The

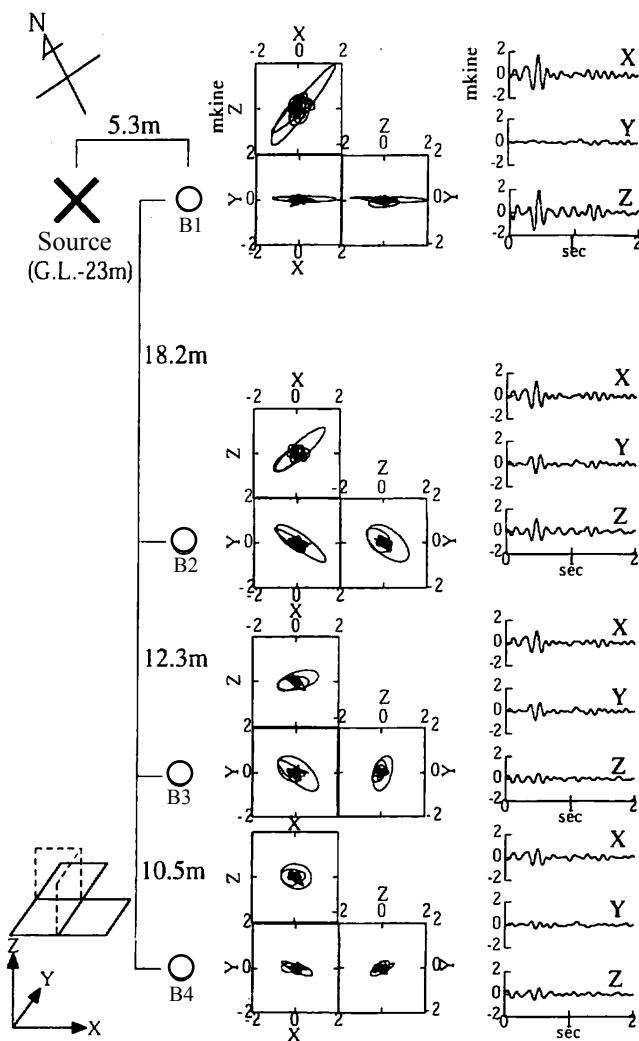Fig.5. Three-dimensional particle motion of observation points on Transect B

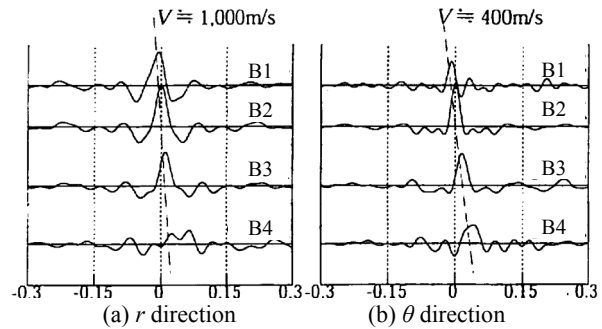(a) r direction   (b) θ direction
Fig.6. Cross correlation functions along Transect B
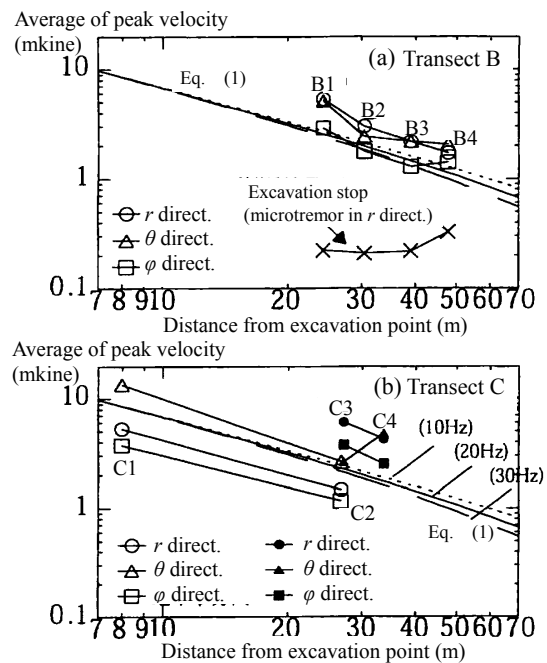

Fig.7. Attenuation of maximum vibration amplitude with distance on Transects B & C

3D particle trajectory is projected onto the X-Y plane, the Y-Z plane and the Z-X plane. In this figure, it can be seen that the direction from any point toward more intense vibration is the same as the direction toward the source of vibration. However, this correspondence between directions is attenuated as the distance from the vibration source increases.

The directions of vibration of the soil particles shown in Fig. 5 were resolved into the r direction toward the source and the θ direction orthogonal to r. The particle motions at points 1 through 4 were analyzed to find waves showing strong mutual correlations in the r and θ directions and propagation in the appropriate order from points B1 to B4. Figure 6 shows cross correlation functions using point B2 as the reference. The wave velocity in the r direction corresponds approximately to the longitudinal wave velocity (1000 m/s), and that for the θ direction, to the transverse wave velocity (400 m/s). These findings show that the vibrations occurring during tunnel

excavation mainly propagate in the form of body waves. This was also noted in the measurements on Transect C.

Figure 7 shows the characteristics of wave attenuation with the average peak velocities observed on Transects B and C. The vertical axis represents the highest mean peak velocity and the horizontal axis represents the distance from the vibration source. The observed values on Transect B were joined with lines in the order B1 – B4, and were compared with the values observed during the machine stops marked by ×. The points on the surface and underground along Transect C are also connected. The theoretical attenuation for body waves,

$$A/A_0 = \exp(-2\pi fhr/V)/r \qquad , \qquad (1)$$

is also plotted here, where A_0 is the vibration amplitude at the source, A is the amplitude at distance r, and f, h and V are the vibration frequency, internal
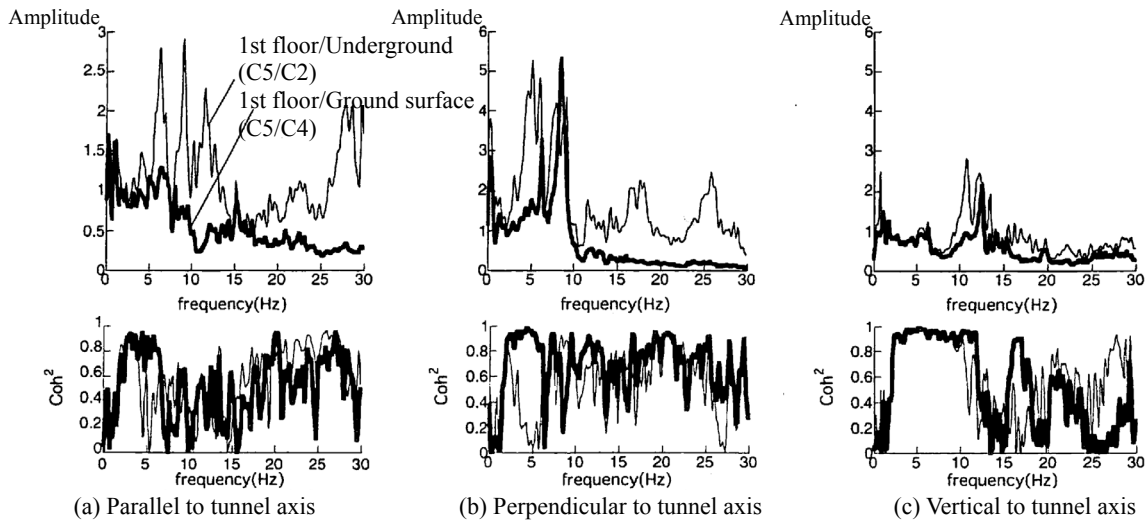

(a) Parallel to tunnel axis (b) Perpendicular to tunnel axis (c) Vertical to tunnel axis

Fig.8. Transfer functions and coherences concerning building containing HVEM

(a) Typical waveform of acceleration on isolation table

(b) EM foundation-table transfer function

a. Isolation rubber
b. EM body
c. Hanging frame
d. Foundation
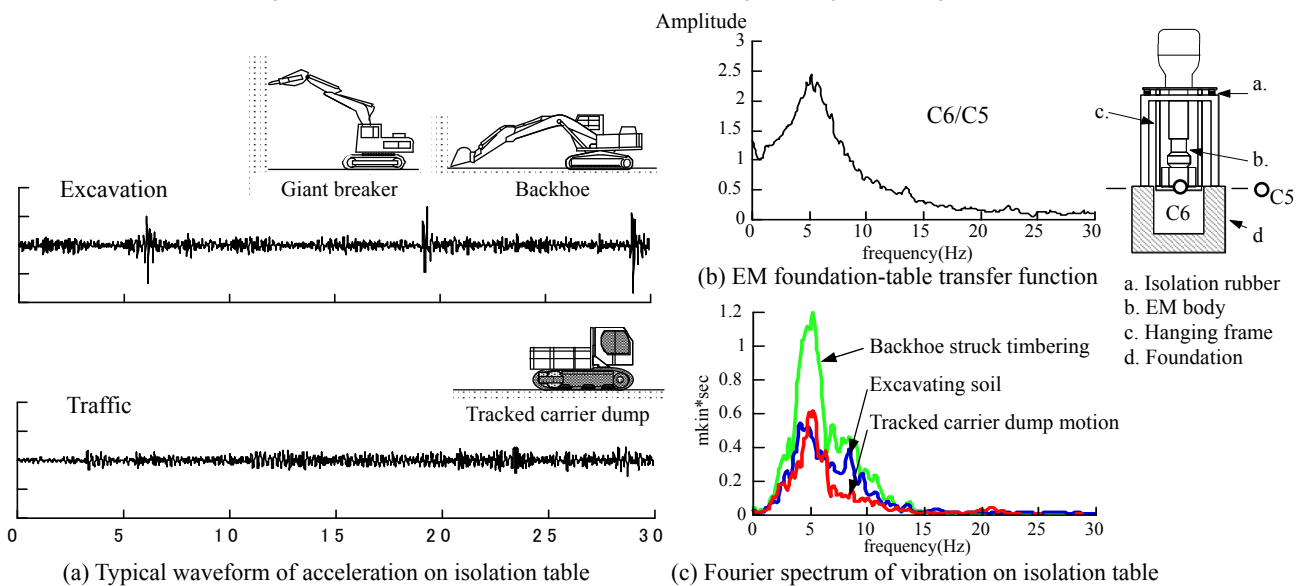
(c) Fourier spectrum of vibration on isolation table

Fig.9. Vibrations experienced by the HVEM installed on an isolation table

damping and elastic wave velocity, respectively. Here, the latter values were $h = 0.02$ and $V = 400$ m/s. These results indicate that, as expected, the main waves were the body waves propagating through the soil. This finding clarified that the attenuation characteristics could be predicted by equation (1) for distance derived for body waves.

5. Vibration Input on Buildings

We will now consider the characteristics of the vibration components propagated through the soil from the tunnel and exerted as forces on buildings. Figure 8 shows the transfer functions in all three dimensions at the foundation of the HVEM on the first floor. Measurements were taken between the underground sensor (C2) along Transect C, under the floor of the HVEM (C5), and at a point between the ground surface (C4) on Transect C and the floor under the HVEM (C5). The horizontal components were considerably amplified at the natural frequency of the building structure, while the higher-frequency components were reduced in the building. Conversely, the vertical vibration did not show significant amplification. The observed attributes of the vibration in this building differed somewhat from those observed in other buildings, although some variation could be expected to arise due to differences in the condition and foundations of the structure of the building.

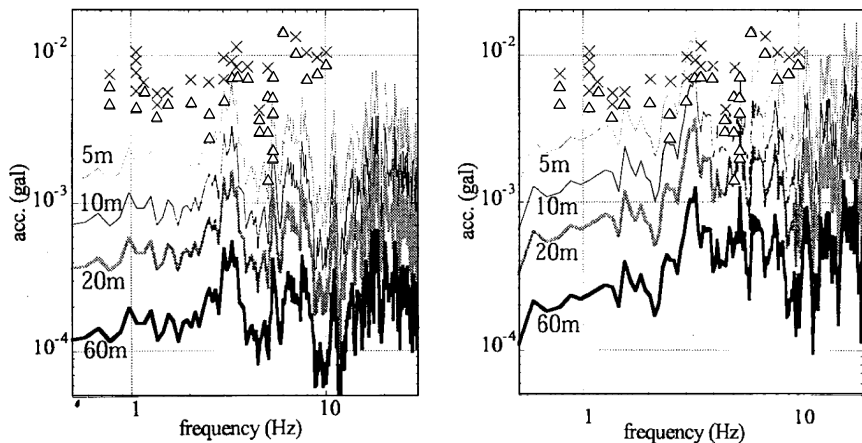## 6. Interference with the Electron Microscope

Figure 9(a) shows the observed waveforms and Fig. 9(c) shows the Fourier spectra of the vibrations excited on the top surface of the vibration isolation table beneath the HVEM. These waves and spectra were predicted by the transfer function between the vibration isolation table and the first floor of the building, as shown in Fig. 9(b). By multiplying the input waves on the first floor of the building (discussed in the previous section) with the transfer function, we able to predict the waveforms and

frequency spectra arriving at the HVEM.

A small shaker for vibration testing was attached to the body of the HVEM and its amplitude and frequency were varied to determine the response in terms of the interference observed on the monitor of the instrument. Figure 10 shows the results of these observations, with the △ symbols in the figure indicating the levels of vibration at which interference was first manifested, and the × symbols showing when interference was clearly present. The four plots show the amplitudes and vibration spectra on the HVEM predicted by the complete set of vibrations associated with the construction activities addressed in this report, including the vibration source characteristics of the operations described in Section 3, the attenuation with distance described in Section 4, the soil to building input characteristics described in Section 5, and the building floor to the isolation table characteristics described in Section 6.

While larger vibrations were detected closer to the source, the observed spectra were frequency dependent. Vibrations were also more intense during excavation of the main tunnel (Fig. 10(b)) compared to construction of the drifts (Fig. 10(a)). The sections of the spectra where the acceleration exceeded the values denoted by the △ symbols indicate where interference occurred in the HVEM at a given distance. The levels of vibration (△) were particularly low at 3 Hz and 5 Hz, indicating increased sensitivity to vibration at those frequencies. Figure 9(b) indicates that 5 Hz was the natural frequency of the HVEM isolation table. Thus, by examining Fig. 10, it was predicted that the HVEM would be disturbed by vibration while excavations were conducted within 60 m of the HVEM for the main tunnel, and within 40 m for the drifts.

Finally, Fig. 11 shows the predicted and observed vibration spectra at the location physically closest to the HVEM. These vibrations exceeded the predicted level resulting in interference to the HVEM at. In addition, the observations confirmed that the images

(a) During excavation of drifts   (b) During excavation of main tunnel
Fig.10. Level of interference due to acceleration of the HVEM (×: Clear interference
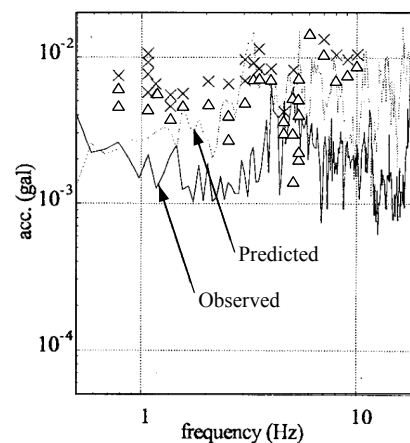△: Not clear) and predicted acceleration spectra for distance from operations

Fig.11. Predicted and observed HVEM acceleration spectra during closest approach of digging operation

provided by the HVEM were affected at this frequency. The reason the observed values were lower than the predicted values was thought to be because the excavation crews had employed measures to mitigate as much vibration as possible, resulting in the predicted results differing only slightly from those obtained from actual observations.

7. Conclusions

This research examined vibrations arising from the excavation of roadway tunnels excavated using the NATM and revealed details about the equipment used for the tunneling work (the sources of the vibrations), the characteristics of the vibrations produced, wave propagation characteristics and their attenuation over distance. The study also examined the vibrations transmitted to buildings, vibratory forces exerted on an HVEM, and the interference to HVEM images. These factors were then combined to predict disturbances to the HVEM before being compared to actual data.

Several innovations were employed in this prediction method; for example, construction activities in the tunnel were monitored using CCTV cameras while the characteristics of the vibrations transmitted between each stage (from the source to the HVEM) were observed with sensors placed underground and in various other locations. This meant that the cause of these vibrations could be determined by observation at the time the disturbances affected the HVEM monitor.

The vibration disturbance predictions were greatly affected by the vibratory characteristics of the excavation activity, the soil, the building and the HVEM. Nevertheless, by applying the methods employed in this study, it will be possible to make accurate predictions of this type in the future. Furthermore, such monitoring methods also allow us to accurately clarify disturbances and damage caused by vibrations.

References

1) Takemiya, H. ed. (2005) Environmental vibrations – Prediction, monitoring, mitigation and evaluation. C.H.I.P.S.
2) Takei, Y., Fujii, K., Izumi, Y. and Nakai, S. (2008) A study on propagation of traffic vibration from tunnel to near building, J. of Environmental Engineering, AIJ, Vol. 73 No. 627, 559-566 (in Japanese)
3) Fukuwa, N., Tobita, J. and Nishizaka, R. (1997) On-line monitoring system for environmental vibration using local area network, J. of Technology and Design, AIJ, No. 5, 158-162 (in Japanese)